GAS DISSOLUTION IN PRESSURIZED HYDRAULIC SYSTEMS – A THEORETICAL APPROACH

Alexander Arch[1] & Dominik Mayr[2]

[1] Generation Technology Conventional / Hydro, EnBW-AG, Germany, Durlacher Allee 93 – 76131 Karlsruhe
[2]Generation High Head Plants, VERBUND Hydro Power AG, Austria, E-Werkstrasse 149, 8121 Deutschfeistritz
E-Mail: a.arch@enbw.com, dominik.mayr@verbund.com

Abstract

The results of calculated dissolution times for a 2 mm air bubble under rising pressure in hydraulic engineering applications are presented. The numerical model was created with Matlab and compared and validated with literature results. The effect of surfactants and turbulence is discussed by applying various approaches for the Sherwood number. Dissolution times for different initial air-saturation concentrations in the water versus the rising pressure along the conduit are presented.

Introduction

Air-water mixtures are comprehensively discussed in chemical engineering processes as well as in hydraulic engineering (e.g. (Vischer & Hager, 1998), (Ahmed & Ervine, 1984), (Ervine, 1998), (Liebermann, 1957), (Falvey, 1980)). By contrast with the situation in chemical engineering, conduit flow in hydraulic engineering is characterized by mean velocities in the range of 1 - 10 m/s, large discharges of > 100 m³/s, diameters > 5 m as well as changing pressures of > 100 bar along the conduits. The initial air saturation is normally unknown, especially for water drawn from a reservoir bottom. In most cases of hydraulic engineering applications air-entrainment in hydraulic systems should be avoided due to negative effects on the mechanical components as well as the hydraulic structures. Free air in pressurized systems also causes detrimental vibrations at the hydraulic machinery or mechanical installations due to dynamic pressure fluctuations. Many studies thus deal with de-aeration in pressurized systems using costly valves or special de-aeration designs. The entrainment of air in a hydraulic system cannot be totally avoided in e.g. collection systems of tributaries within pressurized conduits. In these cases better knowledge of the behavior regarding the dissolution of air-bubbles in water enables adequate reaction by means of well-concerted design changes.

Basic Considerations

The dissolution time of an air-bubble depends on the initial bubble diameter, the velocity at the gas-liquid interface, the water dissolving properties (temperature, contamination, saturation (namely the O_2&N_2 concentration)) and pressure conditions. A common bubble diameter range between 0.5 and 7 mm is noted in technical applications for air entrainment processes ((Chanson, 1996), (Martinez-Bazan, Montanes, & Lasheras, 1999), (Arch, 2008), (Resch & Leutheusser, 1974), (Estrada, 2007)) In turbulent flow regimes bubbles tend to break up and hence are smaller due to shear force effects. The findings of (Clift, Grace, & Weber, 1978), (Levich, 1962), (Spelt & Biesheuvel, 1997), (Salih, 1982) and (Laakkonen, Alopaeus, & Aittamaa, 2002) show mean air-bubble diameters in turbulent flow of between only 1.3 and 3.3 mm. Whether these bubbles will be transported along the pressurized systems or rise against the main flow in an inclined conduit depends on the inclination of the conduit and the liquid discharge. A general assessment of the movement of air in closed conduits was presented by (Falvey, 1980) (Figure 1).

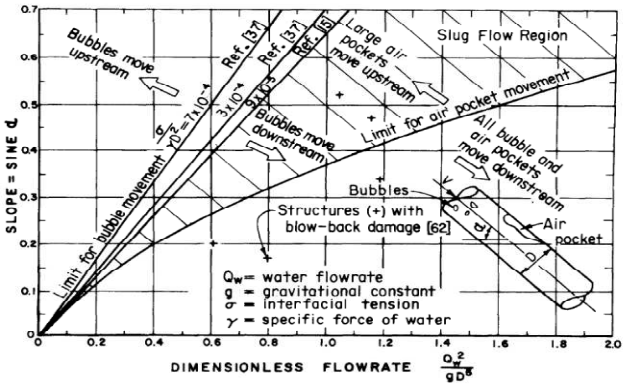

Figure 1: Bubble motion in closed conduits (Falvey, 1980)

Mass transfer is mainly linked to the liquid velocity at the gas-liquid interface (v_{trans}) at the bubble boundary layer (Figure 2). An exact determination for this is a complicated process. In calm water the rise velocity of a single bubble due to buoyancy forces depending on the bubble size will be the determining factor. Turbulence acts on the bubble in conduit flow and together with flow velocities greater than the rise velocity keeps the bubble moving in the main flow direction. The rise velocity of a single bubble in terms of flow field, contamination or the fluid properties has been

widely discussed in (Kulkarni & Joshi, 2005). According to (Hinze, 1975) the minimum turbulence-velocity portion of turbulent pipeline flow is about 3% of the mean velocity. In the present case of air entrainment in inclined hydraulic conduits it is assumed that larger bubbles ($d_B > 2.5$ mm) will remain in the entrainment zone and tend to escape from the turbulent flow field, so that relatively small bubbles only will be transported along the conduit due to turbulence.

In addition mass transfer through the bubble interface depends also on the properties of the surrounding liquid. Surface-active contaminants in liquids accumulate at the bubble surface blocking the interface for diffusion. Studies by (Takemura & Yabe, 1999), (Takemura & Akira, 1998), (Vasconcelos, Orvalho, & Alves, 2002), (Cuenot, Magnaudet, & Spennato, 1997) or (Ponoth & McLaughlin, 2000)) indicate that a bubble in "untreated" water must be considered as bubble with a rigid interface resulting in a lower mass transfer compared with diffusion at a mobile interface, a fact already valid for tap-water conditions.

Beside the gas-liquid interface velocity and the water properties, the initial air saturation concentration in the water has a significant effect on the mass transfer rates and thus the dissolution time. Predicting the saturation concentration in lakes and reservoirs is complex. Depending on the seasonal conditions, water-depth, altitude and ambient temperature various saturation concentrations are found (e.g. (Aho, 1978) and (Ramsey, 1960)). In general the saturation concentration varies between 0 to 90%.

Numerical Model

Theoretical Background

Mass flow rate $\dot{N}$ [mol/s] is calculated acc. to equation (1) where k_{fl} & k_g [m/s] are the coefficients of mass transfer in the liquid phase and the gas-phase respectively, A the bubble surface [m²], ($c^*_{Air\,\infty}$-$c_{Air\,\infty}$) the difference in concentration, R the ideal gas constant [J/mol K], T the temperature [K] and ($p_{Air\,\infty}$ - $p^*_{Air\,\infty}$) the difference in partial pressures (see descriptive Figure 2).

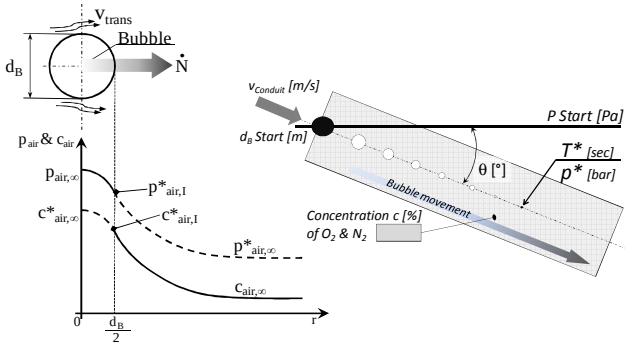

Figure 2: sketch of mass transfer mechanism (left) & main parameters of the numerical simulation (right)

$$\dot{N} = k_{fl} \cdot A \cdot \left(c^*_{Air\,\infty} - c_{Air\,\infty}\right) = \frac{k_g A}{RT}\left(p_{Air\,\infty} - p^*_{Air\,\infty}\right)\left[mol/s\right] \quad (1)$$

According to equation (1) mass transfer can be calculated either related to the gas phase based on the difference in concentrations or - for the process of gas dissolution in liquids - to the liquid phase based on the difference in partial pressures - index *"fl"* represents the fluid and *"g"* the gaseous phase. Both calculations were done within the numerical simulation for verification reasons. The liquid acts as continuous phase which surrounds and flows around the rigid bubble (disperse phase).

Mass transfers coefficients are calculated according to equation (2).

$$k_{fl} = \frac{1}{\frac{1}{\beta_{fl}} + \frac{RT}{\beta_g H_C}} \quad and \quad k_g = \frac{1}{\frac{1}{\beta_g} + \frac{H_C}{RT\beta_{fl}}} \quad (2)$$

Where β_{fl} and β_g are the mass transfer resistances calculated acc. to equation (3) and H_C is Henry's law coefficient.

$$\beta_{fl} = \frac{Sh_{fl} D_{fl}}{d_B} \quad and \quad \beta_g = \frac{Sh_g D_g}{d_B} \quad \left[\frac{m}{s}\right] \quad (3)$$

β_{fl} for the continuous (fluid) and β_g for the disperse (gaseous) phase are depended on the Sherwood number Sh_i [-], the diffusion coefficient D_i [m²/s] and the bubble diameter d_B. After Treybal ((Pflügl & Rentz, 2001)) Sh_g for stationary diffusion in a sphere under rigid conditions can be expressed with equation (4).

$$Sh_g = \frac{2}{3}\pi^2 \quad (4)$$

In the same way as Sh_g also D_{fl} the diffusion coefficient in the fluid phase is in general independent of the ambient pressure but highly dependent on the temperature and can be found in chemical engineering tables. By contrast D_g the diffusion coefficient for the gaseous phase decreases significantly with rising pressure. Based on the findings of Fuller / Schettler / Giddings ((Pflügl & Rentz, 2001)) D_g is calculated according to equation (5) where p is the actual ambient pressure [Pa], MG_{12} the molar mass of the gas ($_1$) & liquid ($_2$) phase [kmol/kg] and v the atomic volume of diffusion.

$$D_g = \frac{1{,}43 \cdot 10^{-7} \cdot T^{1{,}75}}{p \cdot MG_{1,2}^{0.5} \cdot \left[\left(\sum v\right)_1^{\frac{1}{3}} + \left(\sum v\right)_2^{\frac{1}{3}}\right]^2}\left[\frac{m^2}{s}\right]$$
$$with \quad MG_{12} = \frac{2}{\frac{1}{MG_1} + \frac{1}{MG_2}} \quad (5)$$

The liquid-side mass transfer coefficient is expressed in dimensionless form with the Sherwood number Sh_{fl}, and is one of the most important parameters for mass transfer

processes. In many publications an empirical relationship is found for the determination of Sh_{fl}, in the form:

$$Sh_{fl} = C \cdot \mathrm{Re}^{\alpha} \cdot Sc^{1/3} \tag{6}$$

$$\mathrm{Re}_{fl} = \frac{v_{trans} \cdot d_B}{\upsilon_{fl}} \quad and \quad Sc_{fl} = \frac{\upsilon_{fl}}{D_{fl}} \tag{7}$$

where C is a constant (usually between 0.2 and 1.4), Re_{fl} is the Reynolds [-] and Sc_{fl} is the Schmidt number [-] of the fluid phase (equation (7)), power factor α in the order of ½, ν_{fl} is the kinematic viscosity of the fluid phase [m²/s] and v_{trans} the velocity at the gas liquid interface [m/s].

General boundary conditions

In the numerical simulation it is supposed that an air bubble is moved along an inclined conduit with $v_{Conduit}$ due to turbulence effects and thus is exposed to the rising pressure in a similar manner to a water particle moving with the flow. Furthermore it is assumed that the mass of entrained air compared to the mass of the surrounding water is relatively small and thus the overall saturation concentration in the water body does not change during the dissolution process. Isothermal conditions were implied because of the slowness of thermo-dynamic processes.

Based on the findings stated above the initial representative bubble diameter was set to d_B = 2 mm. The bubble diameter will decrease while moving along the conduit due to the effect of gas dissolution in the water and the rising ambient pressure. Depending on the bubble size it is assumed that the interface velocity v_{trans} will either be in the order of the rise velocity of a single bubble (bigger bubble and low flow velocity) or subjected to the turbulence of the entire flow regime in the pipeline (smaller bubble and higher flow velocity). Hence depending on the bubble diameter d_B, the interface velocity v_{trans} was either set to the rise velocity of a single bubble and calculated according to. (Rodrigue, 2004) or - if the turbulence velocity in the conduit is greater than the rise velocity – to 3% of $\cdot v_{Conduit}$.

Since water in reservoirs or tributaries must be regarded as "untreated" the dissolution process in the present case was mainly based on the rigid bubble interface theory. The present numerical simulation applies for concentrations up to 90%, because a single, overall valid saturation concentration of water used in hydraulic infrastructures does not exist. . Air entrainment processes in hydraulic structures usually occur under atmospheric pressure conditions and thus the initial pressure p_{Start} was set to $1.05 \cdot 10^5$ Pa. The temperatures were set to alpine conditions and hence D_{fl} was set to $1.8^{x}10^{-9}$[m²/s] (T = 278 K) in the present simulation.

Against the background of hydro power applications the dissolution time T^* [s] of a single air bubble was calculated for conduit velocities $v_{Conduit}$ from 1 - 10 m/s, conduit angles Θ from 10 - 90° and initial saturation concentration c [%] from 0 to 90 % (percentage in relation to 100% saturation at T = 278 K). A time step of Δt = 0.04 s was chosen. Based on a sensitive analysis of T^* by varying Δt results of T^* with Δt = 0.04 only differ in the order of 10^{-5} which was found acceptable. Material characteristics were taken from (Atkins, 2001) and (Perry & Green, 2008)..

Validation of the numerical model

As stated above the definition of Sh_{fl} is of crucial importance for the diffusion process. Therefore several approaches were tested within the present numerical simulation (equation (8) to (12)). This was done to achieve a better understanding and to describe the process of dissolution in a pressurized conduit accurately against the background of water contamination, interface velocity, turbulence effects and influences due to changing pressure. In the first step the results of the numerical model were compared with an experimental investigation by (Vasconcelos, Orvalho, & Alves, 2002). The authors studied the dissolution process of gas bubbles of different initial diameters in the context of the effects bubble surface contamination has on dissolution behavior in contaminated (run #75) as well as in "clear" water (run #22). The bubbles were kept in place by means of a downward water flow in an experimental setup. Hence the mean velocity at the gas-liquid interface was equal to the rise velocity of the single air bubble which was injected into the flow. As only the initial diameter was mentioned by the authors the velocity v_{trans} had to be calculated. This was done by applying the approach according to (Rodrigue, 2004), which is in very good agreement with rise velocities of single air bubbles measured in tap water.

After Krischer & Kast:

$$Sh_{lam} = 0.664 \cdot \mathrm{Re}^{1/2} \cdot Sc^{1/3} \quad and$$

$$Sh_{turb} = \frac{(0.037 \cdot \mathrm{Re}^{0.8} \cdot Sc)}{(1 + 2.433 \cdot \mathrm{Re}^{-0.1} \cdot (Sc^{2/3} - 1))} \tag{8}$$

$$Sh_{fl-KK} = \sqrt{Sh_{lam}^{\ 2} + Sh_{turb}^{\ 2}}$$

After Rowe:

$$Sh_{fl-Rowe} = 0.79 \cdot \mathrm{Re}^{1/2} \cdot Sc^{1/3} \tag{9}$$

After (Ponoth & McLaughlin, 2000):

$$Sh_{fl-P\&McL} = 0.725 \cdot \mathrm{Re}_{im}^{1/2} \cdot Sc^{1/3} \quad with$$

$$\mathrm{Re}_{im} = \frac{Ar}{18}\left[1 + \frac{Ar/96}{(1 + 0.079 \cdot Ar^{0.749})^{0.755}}\right]^{-1} \quad wherein \tag{10}$$

$$Ar = \frac{d_B^3 \cdot g \cdot \rho_{H2O}^2}{\mu^2}$$

with Ar as Archimedes number [-], g the constant of gravity [m/s²] and μ the dynamic viscosity of the liquid [Ns/m²].

The results of the numerical model in combination with different approaches for Sh_{fl} can be seen in Figure 3 - temperature and saturation concentrations were set to the conditions stated in Figure 3. Starting from an initial bubble diameter of d_B = 8 mm experiment #22u was carried out with so-called "untreated" water, which is comparable to tap water. Applying the approach proposed by (Nguyen, 1998) for calculating the rise velocity in a contaminated liquid, $Sh_{fl\text{-}Rowe}$ showed the most significant agreement. Equations (8) and (9) were taken from (Pflügl & Rentz, 2001).

After (Takemura & Yabe, 1999):

$$Sh_{fl-TY} = \frac{2}{\pi^2}\cdot\left(1-\frac{2}{3}\cdot\frac{1}{(1+0.09\cdot \mathrm{Re}^{2/3})^{3/4}}\right)\cdot\left(2.5+Pe^{1/2}\right) \qquad (11)$$

$$with\ \ Pe=\frac{d_B^3\cdot v_B}{D_{fl}}\ (=Peclet\ number)$$

After (Zhang, J.B., & J.A., 2001):

$$Sh_{fl-Zhang} = \frac{2}{\sqrt{\pi}}\cdot\left(1-\frac{2.89}{\mathrm{Re}^{1/2}}\right)^{1/2}\cdot Pe^{1/2} \qquad (12)$$

Although the transition point to the stagnant cap regime is not reproduced accurately, run #75, which was done in "clean" water (comparable to de-ionised water), could be satisfactorily represented by the approach according to equation (11).

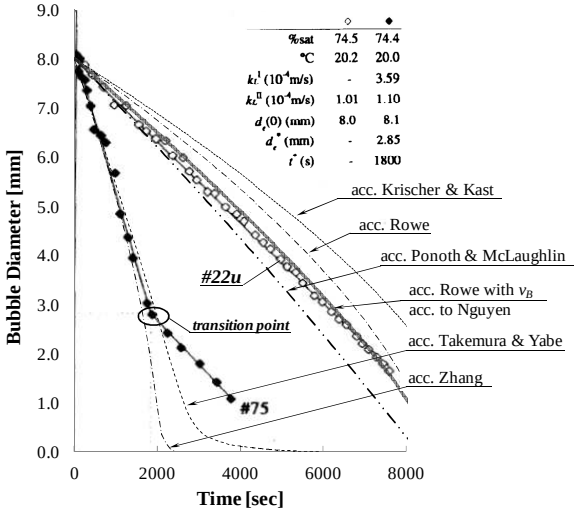

Figure 3: Results of numerical simulation vs. data from experimental investigations by (Vasconcelos, Orvalho, & Alves, 2002); run #75 refers to "clean" water & run #22u to "untreated" water

Studies concerning the dissolution of gas bubbles under turbulent pipeline flow conditions were performed by (Lezhnin, Eskin, Leonenko, & Vinogradov, 2003) and (Kress & Keyes, 1973). Pipe diameters and flow rates in chemical engineering processes are relatively small compared to applications in hydro-power or water supply engineering. Some of the outcomes may thus seem to be valid only for small scale chemical engineering processes.

Based on the energy dissipation by turbulence per unit mass (Avdeev, 1988) - (taken from (Lezhnin, Eskin, Leonenko, & Vinogradov, 2003)) - derived the following promising relationship for the Sherwood number:

$$Sh_{fl-Avdeev} = 0.228\cdot\frac{d_B}{L}\cdot \mathrm{Re}_{tube}^{0.7}\cdot Sc^{0.5} \qquad (13)$$

where Re_{tube} is the Reynolds number of the conduit flow with L as the conduit diameter [m] (equation (14)).

$$\mathrm{Re}_{tube} = \frac{v_{Conduit}\cdot L}{\upsilon_{fl}} \qquad (14)$$

This approach is based on experimental data for bubble liquid mass transfer and also vapor-liquid heat transfer. In Figure 4 and Figure 5 the approaches according to equation (8) and (13) are compared. In the figures the results for dissolution time T^* are shown plotted against κ for different conduit diameters L. The variable κ combines mean velocity $v_{Conduit}$ with conduit angle Θ and represents the pressure change Δp per time unit Δt in [bar/s] and is defined according to equation (15).

$$\kappa = \frac{\Delta p}{\Delta t} = \frac{v_{Conduit}\cdot \sin\Theta}{10.1972}\left[bar/s\right] \qquad (15)$$

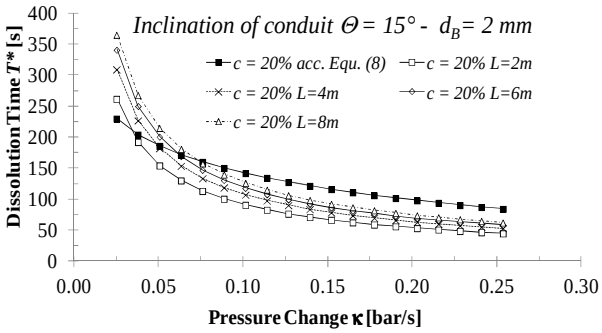

Figure 4: Comparison between equation (8) and equation (13) at constant conduit angle of Θ = 15° and c = 20 % - different conduit diameters L applied

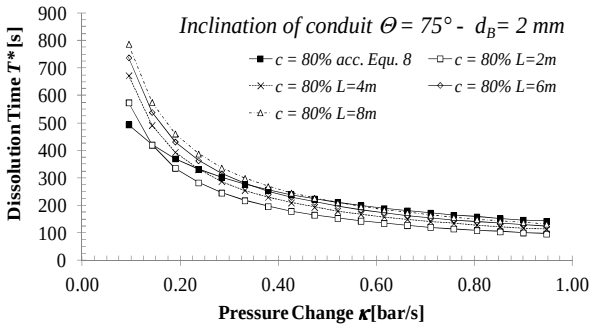

Figure 5: Comparison between calculated dissolution time T^* according to equation (8) and equation (13) at constant conduit angle of Θ = 75° and c= 80 % - different conduit diameters L applied

Applying equation (13) lower dissolutions times T^* are found for higher velocities $v_{Conduit}$ compared to the approach

of Krischer & Kast. In contrast to a fixed turbulence level of 3% in the numerical model, the minimal turbulence level will increase to more than 3 % with increasing conduit velocity $v_{Conduit}$ in small scale applications with the effect of higher mass transfer rates. At the lower end (κ = 0 to 0.2), where $v_{Conduit}$ is relatively small (~1 m/s), mass transfer rates are much lower according to (Avdeev, 1988) than when applying equation (8). Although equation (8) represents laminar as well as turbulent boundary layer conditions the turbulence of the conduit flow seems to act less on the interface boundary compared to the buoyancy forces for the tube diameters applied. (Lezhnin, Eskin, Leonenko, & Vinogradov, 2003) stated that there is a lack of experimental data and due to the scattered results obtained more physical investigations are needed. Due to the fact that equation (8) produces more conservative results for T^* for higher velocities and low velocities ($v_{Conduit}$ < 1.5 m/s) are rarely found in pressurized systems, it was decided to apply equation (8) in the numerical model.

Results and Discussion

According to Figure 6 dissolution time T^* rises with increasing saturation concentration c, decreasing conduit velocity $v_{Conduit}$ and decreasing conduit inclination Θ.

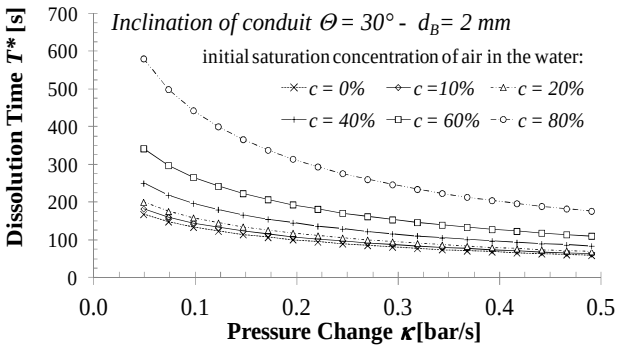

Figure 6: Dissolution time T^* for different initial saturation concentrations c for a constant conduit angle of θ = 30° and initial bubble diameter d_B = 2 mm

Increasing conduit velocity $v_{Conduit}$ leads to lower dissolution time T^* due to higher mass transfer rates (Figure 6). As turbulence plays a more important role at higher velocities compared to the rise velocity of a single bubble v_{trans} at the gas-liquid interface increases. Regarding a 2 mm air-bubble T^* is in the range of 50 to 700 seconds applying saturation concentrations from 0 to 80% (Figure 7 to Figure 9). The results for $T^*_{90°}$ (vertical arrangement of the conduit (pressure shaft)) only differ in the order of 0.5 to 2 seconds from the results for $T^*_{75°}$. Therefore the graphs for Θ = 75° can be used for applications with Θ = 90°. As can be seen in Figure 7 the pureness of water has a certain effect on the dissolution process. On average T* is at least doubled when acting under "untreated" conditions. As stated above, the "untreated" approach according to equation (8) is more likely to meet conditions in hydro-power systems as well as in the domain of water supply.

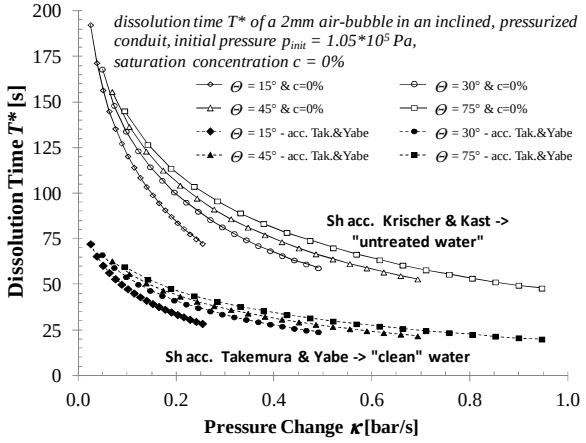

Figure 7: Dissolution time T^* for several conduit angles against pressure change κ for c = 0%- comparison of results for "clean" and "untreated" water – d_B = 2mm

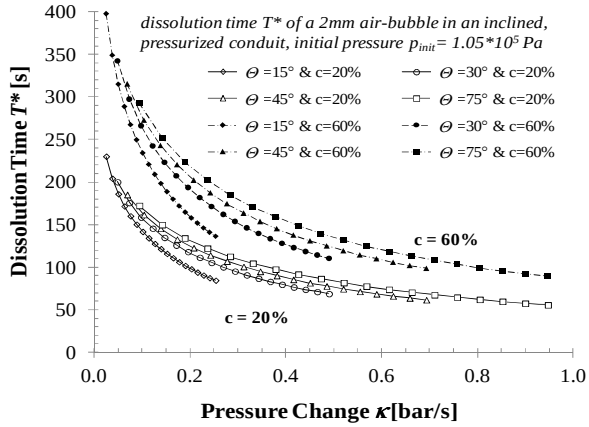

Figure 8: Dissolution time T^* for several conduit angles plotted against κ for c = 20% & 60%- d_B = 2mm

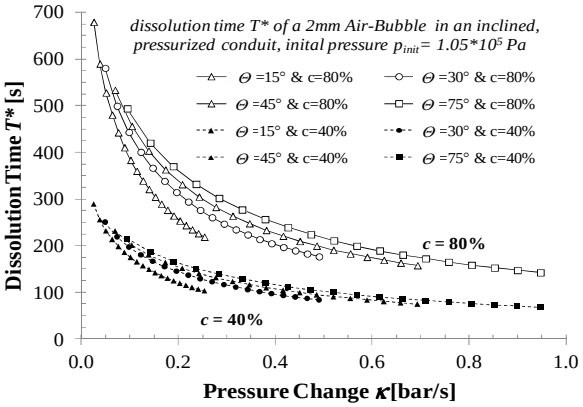

Figure 9: Dissolution time T^* for several conduit angles plotted against κ for c = 40% & 80% - d_B = 2mm

Figure 10 shows the normalized results of T^* for clean and untreated conditions. A first rough assessment of the dissolution time in pure systems might be made by

applying the relationship from Figure 10 based on values for T^* from Figure 7 to Figure 9.

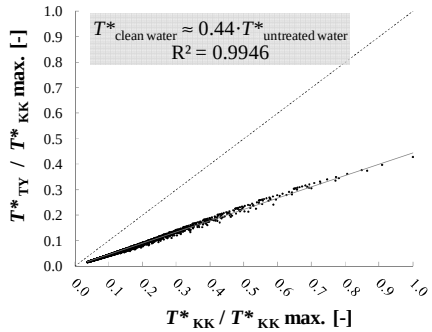

Figure 10: Comparison of clean (TY) and untreated (KK) results of T^* according to equation (11) and (8)

Conclusion & Outlook

Based on a regression analysis T^* against κ follows in general the relationship:

$$T_i^* = C_1 \cdot \ln(\kappa) + C_2 \tag{16}$$

The coefficients C_1 and C_2 are dependent on the conduit angle Θ, the initial concentration c and the bubble diameter d_B. For a first assessment of the dissolution time T^* the graphs presented can be used. In the next steps a general relationship for calculating T^* will be elaborated by solving equation (9) for different Θ and saturation concentrations c. Based on prototype measurements for the distribution of d_B in air-entrainment processes according to (Mayr, Arch, & Winkler, 2006) concentration profiles along the conduit will be elaborated.

References:

Ahmed, A. A., & Ervine, D. A. (1984). The Process of Aeration in closed Conduit Hydraulic Structures. *Symposium on scale effects in modelling hydraulic structures.* Esslingen am Neckar.

Aho, J. (Vol. 15 1978). Winter oxygen content in relation to water temperature and duration of ice cover in southern Finland. *Ann. Zool. Fennici*, S. 1-7.

Arch, A. (2008). *Luftein- und Austragsprozesse bei Anlagen mit Peltonturbinen im Gegendruckbetrieb.* Schriftenreihe zur Wasserwirtschaft - Vol.52: Technische Universität Graz.

Atkins, P. W. (2001). *Pysikalische Chemie.* 3. Auflage: WILEY-VCH.

Avdeev, A. A. (1988). Laws of Groth, Condensation and Dissolution of Vapor and Gas Bubbles in Turbulent Flows. *High Temperature*, S. 214-220.

Chanson, H. (1996). *Air Bubble Entrainment in Free-Surface Turbulent Shear Flows.* Academic Press.

Clift, R., Grace, J. R., & Weber, M. E. (1978). *Bubbles, Drops and Particles.* Academic Press.

Cuenot, B., Magnaudet, J., & Spennato, B. (Vol. 339 1997). The effects of slightly soluble surfactants on the flow around a spherical bubble. *J. Fluid Mech.*, S. 25-53.

Ervine, D. A. (vol. 130 1998). Air Entrainment in Hydraulic Structures: A Review. *Proc. Instn Civ. Engr Wat., Marit. & Energy*, S. 142 - 153.

Estrada, O. P. (2007). *Investigation on the Effects of Entrained Air in Pipelines.* Stuttgart: Mitteilungen des Institutes für Wasserbau, Universität Stuttgart, Vol. 158.

Falvey, H. T. (1980). *Air-Water Flow in Hydraulic Structurs.* United States Department of Interior: Engineering Monograph No. 41.

Hinze, J. O. (1975). *Turbulence.* McGraw-Hill.

Kress, T. S., & Keyes, J. J. (Vol. 28 1973). Liquid phase controlled mass transfer to bubbles in cocurrent turbulent pipeline flow. *Chem. Engineering Science*, S. 1809-1823.

Kulkarni, A. A., & Joshi, J. B. (Vol. 44 2005). Bubble Formation and Bubble Rise Velocity in Gas-Liquid Systems: A Review. *Ind. Eng. Chem. Res.*, S. 5873-5931.

Laakkonen, M., Alopaeus, V., & Aittamaa, J. (2002). *The Determination of Parameters for Bubble Breakage and Coalescence Functions for Gas-Liquid Systems in a mixed Tank.* Indianapolis, US: Annual Meeting Archive - American Institute of Chemical Engineers.

Levich, V. G. (1962). *Physicochemical Hydrodynamics.* Prentice-Hall International Series.

Lezhnin, S., Eskin, D., Leonenko, Y., & Vinogradov, O. (Vol. 39 2003). Dissolution of air bubbles in a turbulent water pipeline flow. *Heat and Mass Transfer*, S. 483-487.

Liebermann, L. (No. 2. Vol. 28 1957). Air Bubbles in Water. *Journal of Applied Physics*, S. 205-211.

Martinez-Bazan, C., Montanes, J. L., & Lasheras, J. C. (Vol. 401 1999). On the breakup of an air bubble injected into a fully developed turbulent flow. Part 2. Size PDF of resulting daughter bubbles. *Journal of Fluid Mechanics*, S. 183-207.

Mayr, D., Arch, A., & Winkler, M. (2006). Prototyp Measurements of De-Aeration in subcritical Flows. *International Symposium of Hydraulic Structures* (S. 1-12). Ciudad Guayana, Venezuela: IAHR.

Nguyen, A. V. (No. 1. Vol. 44 1998). Prediction of Bubble Terminal Velocities in Contaminated Water. *AIChE Journal*, S. 226 - 230.

Perry, R. H., & Green, D. W. (2008). *Perry's Chemical Engineers' Handbook - 8th Edition.* McGraw-Hill.

Pflügl, M., & Rentz, A. (2001). *Stoffaustausch* (5. Ausg.). Institut für Grundlagen der Verfahrenstechnik und Analgentechnik: Techn. Univ. Graz.

Ponoth, S. S., & McLaughlin, J. B. (Vol.55 2000). Numerical Simulation of mass transfer for bubbles in water. *Chemical Engineering Science*, S. 1237 - 1255.

Ramsey, W. L. (Vol. 5 (1) 1960). Dissolved Oxygen in Sweetwater Lake. *American Society of Limnology and Oceanography*, S. 34-42.

Resch, F. J., & Leutheusser, H. J. (Issue 100. Proceedings of the ASCE 1974). Bubbly two Phase Flow in Hydraulic Jump. *Journal of hydraulic Devision*, S. 137-149.

Rodrigue, D. (Issue 2. Vol.82 2004). A General Correlation for the Rice Velocity of single Gas Bubbles. *Ca. J.. Chem. Eng.*, S. 382-386.

Salih, A. A. (1982). Size distribution of air bubbles entrained in accelerated turbulent water flow. *BHRA Fluid Engineering - Hydraulic Modelling of Civil Engineering Structures*, S. 223-235.

Spelt, P. M., & Biesheuvel, A. (Vol. 336 1997). On the motion of Gas Bubbles in homogeneous, isotropic Turbulence. *Journal of Fluid Mechanics*, S. 221-244.

Takemura, F., & Akira, Y. (No. 15. Vol. 52 1998). Gas dissolution process of spherical rising gas bubbles. *Chemical Engineering Science*, S. 2691-2699.

Takemura, F., & Yabe, A. (Vol. 378 1999). Rising speed an dissolution rate of a carbon dioxide bubble in slightly contaminated water. *J. Fluid Mech.*, S. 319 - 334.

Vasconcelos, J. M., Orvalho, S. P., & Alves, S. S. (No. 6. Vol. 48 2002). Gas-Liquid Mass Transder to Single Bubbles: Effect of Surface Contamination. *AIChE Journal - Fluid Mechanics and Transport Phenomena*, S. 1145 - 1154.

Vischer, D. L., & Hager, W. R. (1998). *Dam Hydraulics.* John Wiley & Sons.

Zhang, Y., J.B., M., & J.A., F. (Vol. 56 2001). Bubble velocity profile and model of surfactant mass transferto bubble surface. *Chemical Engineering Science*, S. 6605 - 6616.